FEMANOLA v3.0 as a Tool to Predict Settlement-Induced Cracks in Masonry Walls

Natalia Pingaro(✉) and Gabriele Milani

Department of Architecture, Built Environment and Construction Engineering, Politecnico di Milano, 20133 Milan, Italy
natalia.pingaro@polimi.it

Abstract. This paper introduces a finite element tool (FEMANOLA v3.0) developed for the nonlinear analysis of masonry walls subjected to ground settlements. The approach, specifically conceived for masonry structures, uses a heterogeneous modeling technique, i.e. bricks and mortar are meshed separately. In particular, bricks are modeled using elastic four-node elements, while mortar joints are represented as nonlinear interfaces with cohesive-frictional behavior, incorporating softening in tension and compression under the application of shear actions. Mortar interfaces are discretized through isogeometric four-node elements, ensuring that normal stresses along the interface direction are nullified. The reliability and precision of the model are verified by comparing the results obtained with some available in the existing literature, focusing on masonry walls subjected to settlement. These comparisons highlight the model ability to accurately predict the response of masonry walls subjected to ground settlement, including crack initiation, propagation, and failure mechanisms. FEMANOLA v3.0 thus provides a robust and efficient strategy for analyzing masonry structures subjected to settlement, offering key insights into the performance and failure mechanisms of historical masonry walls under various load conditions.

Keywords: Masonry · Settlement · FE analysis · Nonlinear interfaces

1 Introduction

The necessity of preserving historical masonry buildings has heightened interest in studying this type of construction. This has caused the need to develop new and appropriate computational methods to analyze their structural performance. A significant part of this area involves understanding the reasons behind the damage observed in existing structures. Although masonry buildings are highly vulnerable to horizontal forces [1–3], cracks can still be found in structures located in non-seismic regions or areas without a history of seismic activity. Given that the equilibrium state of a masonry structure primarily depends on its geometry [4–8], one of the contributors to damage is the motion of its foundations [9–13]. In many cases, the formation of cracks is attributed to differential settlements. It is important to note that most old masonry buildings were originally constructed on foundations composed of various structural elements, often

© The Author(s), under exclusive license to Springer Nature Switzerland AG 2026
O. Gervasi et al. (Eds.): ICCSA 2025 Workshops, LNCS 15886, pp. 396–409, 2026.
https://doi.org/10.1007/978-3-031-97576-9_27

disconnected from one another. Therefore, when soil motion occurs, the upper structure experiences differential displacements at the base level, leading to a deformed equilibrium configuration.

The existing technical literature provides various studies that address the development of crack patterns due to foundation settlements. Many of these works analyze the issue by performing nonlinear simulations using the Finite Element Method (FEM). In some models, the soil-structure interaction is explicitly included by modeling the soil itself [14]. In [15] the authors propose a 2D semi-coupled FEM model that incorporates this interaction through dedicated soil-structure interfaces. After validating the model through experimental tests [15], they apply it to analyze a façade subjected to settlement caused by tunneling [16]. In general, many studies opt to simplify the modeling of the soil to reduce computational complexity, often simulating settlements by directly applying displacements at the base of the numerical model. Some research uses nonlinear FEM to study the effects of settlements on masonry arch bridges [17] or to assess how structural modifications might influence the occurrence of differential settlements in historical masonry buildings [18]. This approach is sometimes enhanced with homogenization techniques [19].

As an alternative to FEM, some studies use the Distinct Element Method (DEM) [20, 21], or iterative analyses on macro-blocks with nonlinear springs at their interfaces [22, 23]. Other studies idealize the masonry structure as an assembly of rigid blocks, identifying crack patterns through limit analysis procedures that are solved using linear and conic programming techniques [24–29]. The latter are particularly suitable for representing the behavior of masonry structures under settlement.

Nevertheless, all the aforementioned numerical procedures are not without drawbacks. Commercial FEM codes can be complex for common users, for whom obtaining reliable results is not a straightforward task, primarily because the material models available in the standard libraries of commercial software—potentially adaptable to handle such sources of nonlinearity—are typically designed for other application contexts. At the same time, DEM models, while requiring fewer parameters than FEM and concentrating cracks at the interfaces between blocks, do not allow for heterogeneous modeling, and nonlinear static analyses are, in fact, slow dynamic analyses. Finally, limit analysis, while being the most suitable for a settlement-induced cracking problem in masonry, overestimates the ultimate load-bearing capacity, classical limit analysis does not account for sliding and, if yes, it is associated, and the blocks are rigid therefore the deformed shape is all inelastic. Consequently, limit analysis becomes predictive only in proximity to the development of a well-defined kinematic chain.

Unfortunately, dedicated software still appears to be lacking in the literature, and the present paper aims to fill this gap. FEMANOLA v3.0, which stands for Finite Element MAsonry NOn Linear Analysis, is a 2D Finite Element homemade code implemented to carry out nonlinear static analyses for masonry structures subjected to plane loads. The material behavior is represented through a heterogeneous approach, with nonlinearity concentrated in the joints, modeled as interfaces. A key feature of the code is that the joints can be meshed with either their actual thickness or an almost negligible thickness (to represent interfaces or dry joints). In both cases, the joints are represented using four-node isoparametric elements, with the elastic modulus in their direction assumed to be

zero. The blocks are considered elastic and are discretized again using standard four-node isoparametric elements. The software is capable of handling both plane deformation and plane stress analyses. The material model for the joints incorporates coupled shear and normal stress behavior. A cohesive frictional model is applied for shear, with the joint undergoing progressive damage once the peak shear stress is reached. The post-peak tangential behavior is governed by a user-defined Mode II fracture energy, which is assumed to depend on the current normal stress. A residual strength, also defined by the user concerning the normal stress, can be incorporated as well. The nonlinear solver follows an iterative elastic scheme [30–34], where the stiffness of Gauss points exhibiting softening is penalized using a straightforward return-to-limit-surface algorithm that is entirely explicit. The robustness of the solver is improved in the presence of softening, facilitating rapid nonlinear analyses without the risk of premature failure. The accuracy of the results is ensured when sufficiently small load increments are applied. Since arc length control is not yet available, analyses can be performed under displacement control.

The numerical method proposed offers several advantages over conventional commercial codes, the most notable of which is the wealth of information (particularly at the local level) available during post-processing. Among the numerous case studies used to validate the reliability of the internally developed software, only one is presented here for brevity. This case involves a masonry wall subjected to settlement, previously examined both experimentally and numerically in [35, 36]. Excellent predictive capabilities are demonstrated in replicating experimental tests at both global and local levels.

2 FEMANOLA v3.0 Description

This section aims to present a new in-house developed nonlinear static Finite Element (FE) software (named FEMANOLA v3.0), where the material nonlinearity is managed using a fully explicit iterative elastic approach. For the mortar joints, four-node isoparametric elements are employed, with the normal stiffness in the direction of the joint being set to zero. The joints can be meshed either with their actual thickness or with an almost negligible thickness to simulate interfaces or dry joints. This allows the interfaces, with their specific geometric thickness, to be modeled in the pre-processing phase in the same manner as a standard elastic heterogeneous discretization. The model assumes plane stress conditions, although plane-strain problems can also be analyzed.

Since nonlinearity is addressed through an elastic procedure that progressively reduces the stiffness of damaged Gauss points to account for softening, it is useful to refer to the elastic case directly, where $\mathbf{D}$ represents the elastic stiffness of the mortar joint.

Consider a local coordinate system for each mortar joint, as shown in Fig. 1, where x′ and y′ correspond to the local axes aligned with the direction of the joint and its normal, respectively. It is also assumed that t_E is the out-of-plane thickness of the element (considered constant), $\mathbf{J}$ is the Jacobian of the transformation from physical to natural coordinates (ξ_1 and ξ_2), and $\mathbf{B}$ is the matrix that contains the first derivatives of the shape functions. Therefore, the element stiffness matrix in the local coordinate system is given by:

$$\mathbf{K'}_E = \int_{-1}^{1}\int_{-1}^{1} \mathbf{B^T D B}|\mathbf{J}|t_E d\xi_1 d\xi_2 \tag{1}$$

A standard integration using four Gauss points is employed, enabling the numerical evaluation of $\boldsymbol{K'}_E$ as follows:

$$\mathbf{K'}_E = \sum_{\mathrm{i}=1}^{4} \mathrm{w_i}\mathbf{B_i}^{\mathrm{T}}\mathbf{D_i}\mathbf{B_i}|\mathbf{J_i}| = \text{Gauss Point} \tag{2}$$

where $\mathrm{w_i}$ represent the weights of the Gauss points.

Finally, a rotation $\boldsymbol{R}_{-\vartheta_E}$ is performed to obtain the element stiffness matrix in the global coordinate system:

$$\mathbf{K}_E = \mathbf{R}_{-\vartheta_E}{}^T \mathbf{K'}_E \mathbf{R}_{-\vartheta_E} \tag{3}$$

The elastic stiffness matrix $\mathbf{D}$ of the element is assumed to be diagonal, with the normal component along the direction of the joint set to zero:

$$\mathbf{D_i} = \begin{bmatrix} 0 & 0 & 0 \\ 0 & E^{k,i} & 0 \\ 0 & 0 & G^{k,i} \end{bmatrix} \tag{4}$$

where $E^{k,i}$ and $G^{k,i}$ denote the Young's modulus and shear modulus of the mortar at the i-th Gauss point during the k-th iteration of the loading process, respectively.

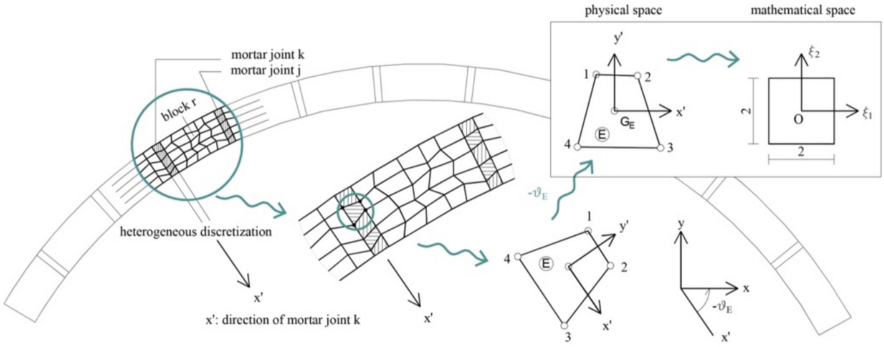


Fig. 1. Heterogeneous finite element discretization of a masonry structure in FEMANOLA v3.0.

Concerning non-linearity, its general aspects are illustrated in Fig. 2, which specifically represents the response of a Gauss point subjected to inelastic tensile stress. Suppose that, at the end of the load iteration k, the i-th Gauss point experiences normal stress $\sigma_{nn}^{k,i}$ that exceeds its tensile strength. Notably, if the Gauss point is already on the softening branch, this strength is lower than its initial undamaged value. In such a case, the elastic modulus for the next iteration k + 1 is adjusted according to the return mapping scheme shown in Fig. 2. Since the procedure is fully explicit, no sub-iterations are required,

ensuring convergence as long as the external load is applied in sufficiently small increments. Typically, instead of imposing forces, displacements are progressively increased to explicitly capture the structural response in the softening phase.

The constitutive model for the joint distinguishes between tensile, compressive, and shear behavior. This is defined during preprocessing through a user-friendly Excel spreadsheet interface, as depicted in Fig. 3, where the mechanical parameters required to set up the model are shown. The code does not include purely numerical parameters (such as the viscosity one in the CDP model in Abaqus); instead, every property set in FEMANOLA v3.0 corresponds to a clear physical counterpart. It is interesting to point out that the number of mechanical parameters required by a numerical code is directly proportional to the information that can be obtained in the output. Therefore, a greater number of mechanical parameters corresponds to a more detailed representation of the physical behavior in the numerical model.

2.1 Tensile Behavior

The tensile behavior consists of an initial elastic phase (with Young's modulus E and peak tensile strength f_t), followed by an exponential softening governed by fracture energy G_I^f and described by the following equation:

$$\begin{aligned} &\varepsilon_{nn} < f_t/E \qquad \sigma_{nn} = E\varepsilon_{nn} \\ &\varepsilon_{nn} \geq f_t/E \; \sigma_{nn} = f_t e^{-\frac{\varepsilon_{nn} - f_t/E}{G_I^f}} \end{aligned} \tag{5}$$

where ε_{nn} represents the normal strain.

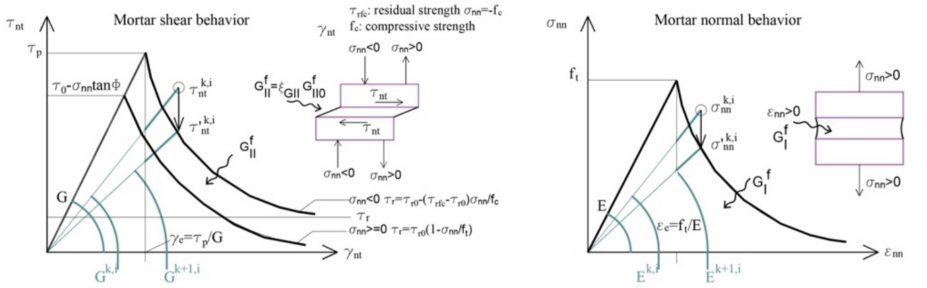


Fig. 2. Penalization scheme for the elastic and shear moduli of a Gauss point undergoing softening in tension (right) and shear (left).

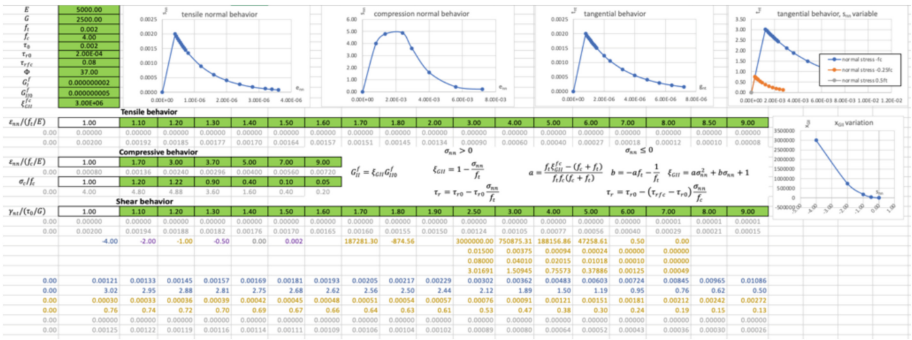


Fig. 3. Excel spreadsheet interface for defining the constitutive behavior of mortar joints (using the data employed to obtain the numerical results in Sect. 3).

2.2 Compressive Behavior

Unlike the tensile behavior, the compressive response is defined through discrete points to accurately capture the typical hardening-softening behavior of a mortar joint under compression. f_c denotes the stress at the elastic limit, while the elastic modulus remains the same as in the tensile regime.

It is important to note that, within the context of FEMANOLA v3.0, it is feasible to study the case of a material with no tensile resistance. Even though zero tensile strength cannot be directly implemented, a very low tensile resistance and similarly low fracture energy can approximate a no tension scenario. As a result, the compressive resistance is not activated. However, there is the possibility to account for joint crushing if needed, but this is not relevant in the current case, as will be demonstrated in the validation section.

2.3 Shear Behavior

The shear behavior is characterized by a linear-exponential $\tau_{nt} - \gamma_{nt}$ relationship (see Fig. 4), coupled with the normal stress σ_{nn} acting on the interface. This interaction is governed by a cohesive frictional law. In Fig. 4, n represents the unit normal vector of the interface, and t refers to the interface direction.

For a given normal stress σ_{nn}, let Φ, τ_0, and τ_{r0} denote the friction angle, tensile peak, and residual strengths at $\sigma_{nn} = 0$, , respectively. The peak (τ_p) and residual (τ_r) tangential strengths for any applied σ_{nn} are given by the following relations:

$$\begin{gathered} \tau_p = \tau_0 - \sigma_{nn} tan\Phi \\ \sigma_{nn} < 0 \rightarrow \tau_r = \tau_{r0} - \left(\tau_{rfc} - \tau_{r0}\right)\frac{\sigma_{nn}}{f_c} \\ \sigma_{nn} \geq 0 \rightarrow \tau_r = \tau_{r0} - \tau_{r0}\frac{\sigma_{nn}}{f_t} \end{gathered} \tag{6}$$

The $\tau_{nt} - \gamma_{nt}$ relationship is hence defined as follows, distinguishing between elastic and inelastic softening phases:

$$\begin{gathered} \gamma_{nt} < \tau_p/G \qquad\qquad \tau_{nt} = G\gamma_{nt} \\ \gamma_{nt} \geq \tau_p/G \;\; \tau_{nt} = \left(\tau_p - \tau_r\right)e^{-\frac{\gamma_{nt} - \tau_p/G}{G_{II}^f}} + \tau_r \end{gathered} \tag{7}$$

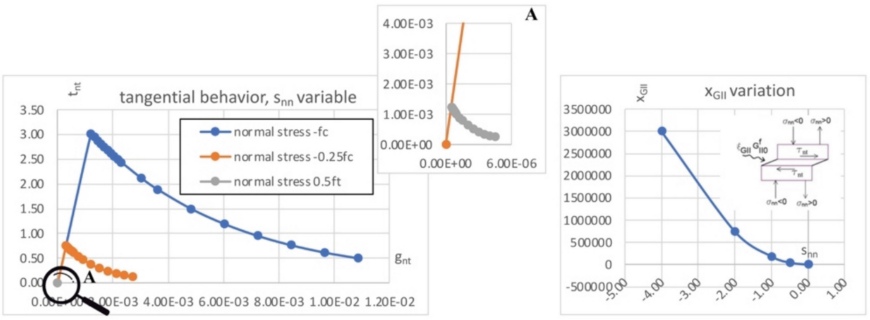


Fig. 4. Shear response of the mortar joints under varying normal stress levels σ_{nn} (left) and the non-dimensional parameter ξ_{GII} used to adjust the Mode II fracture energy at different σ_{nn} levels (right).

where G_{II}^f denotes the Mode II fracture energy, G is the shear modulus, and all other symbols have already been defined. In the model, G_{II}^f is also assumed to be dependent on σ_{nn} as described by the following relationship:

$$G_{II}^f = \xi_{GII} G_{II0}^f \tag{8}$$

where G_{II0}^f represents the Mode II fracture energy at $\sigma_{nn} = 0$, and ξ_{GII} is a non-dimensional parameter that increases parabolically when $\sigma_{nn} \leq 0$ and decreases linearly when $\sigma_{nn} > 0$, as given by the following formulas:

$$\begin{gathered} \sigma_{nn} \leq 0 \rightarrow \xi_{GII} = a\sigma_{nn}^2 + b\sigma_{nn} + 1 \text{ where } a = \frac{f_t \xi_{GII}^{fc} - (f_c + f_t)}{f_t f_c (f_c + f_t)} \; b = -af_t - \frac{1}{f_t} \\ \sigma_{nn} > 0 \rightarrow \xi_{GII} = 1 - \frac{\sigma_{nn}}{f_t} \end{gathered} \tag{9}$$

3 FEMANOLA v3.0 Validation on a Masonry Wall Subjected to Settlement

To validate the effectiveness of the proposed approach, experimental and numerical results from the literature are used, as referenced in [35, 36].

The benchmark is a masonry dry-joint wall whose dimensions are 1737 × 605 × 90 mm^3. A uniform downward displacement is imposed at the bottom-right corner, over a length equivalent to 190% of a single brick length (as illustrated in Fig. 5).

Figure 6 presents the load-displacement curves plotted for nodes 771, 733, 783, 735, and 212, where unit displacements are applied (as shown in Fig. 5). At nodes 771, 783, and 212, the reaction force is nearly zero, as confirmed by the graph in Fig. 6, where the three corresponding curves overlap almost perfectly at the origin. The most significant reaction forces are observed at nodes 733 and 735, which are approximately located at the centroid of the two blocks (see the zoom provided in Fig. 6). The reaction force at node 735 is larger than that at node 733 because the two forces form a couple, ensuring a constant displacement to prevent rotation as depicted in the zoom provided in Fig. 6.



Fig. 5. The masonry wall under study.

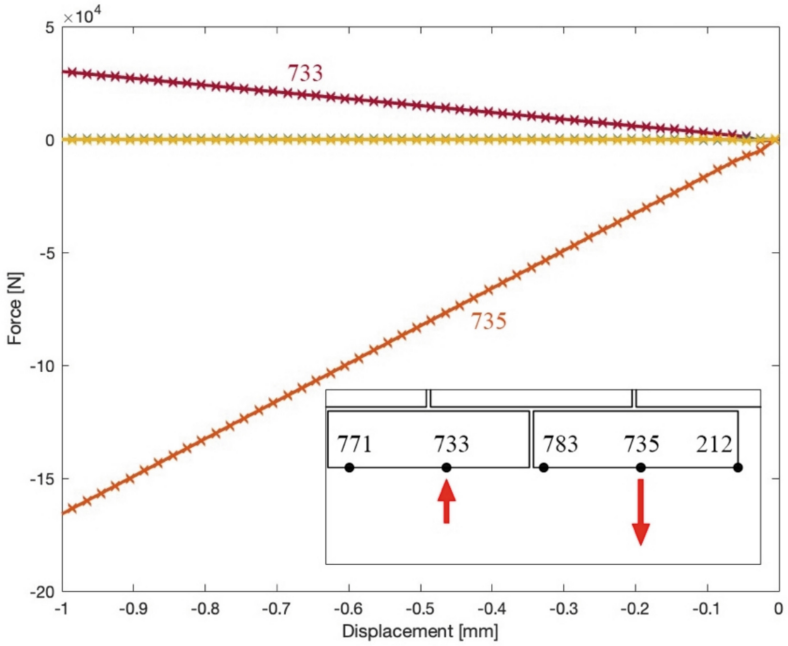


Fig. 6. Force-displacement curves obtained in the five nodes in which the unitary displacements are applied.

Figures 7 and 8 illustrate the local behavior at step 13 out of 50, presenting tangential and normal stresses. Additionally, the shear and tensile damage states are also shown.

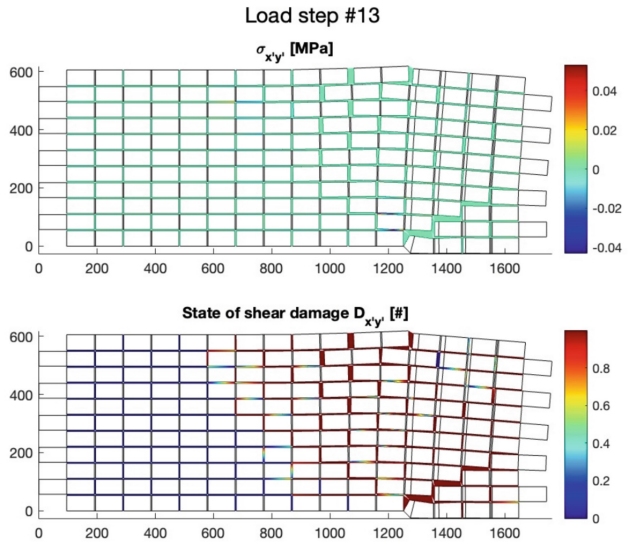


Fig. 7. Local behavior (step #13). Tangential stresses and state of shear damage.

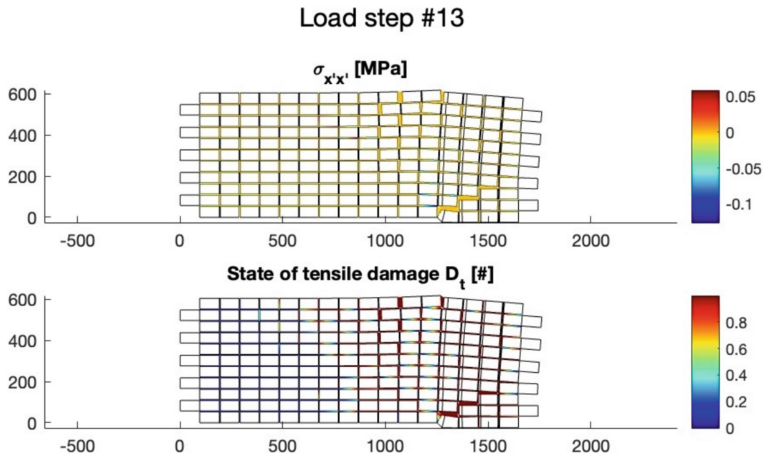


Fig. 8. Local behavior (step #13). Normal stresses and state of tensile damage.

The same results are reported in Figs. 9 and 10 for step 50.

In Fig. 11 a zoom of Fig. 10 regarding the state of tensile damage is shown.

In conclusion, it can be observed that in the figures corresponding to step 13, damage is developing, primarily concentrated in the area where displacements are applied. The evolution of the global failure mechanism becomes evident in step 50 and aligns with the numerical results from limit analysis found in [36] and with experimental evidences [35]. Additionally, Figs. 10 and 12 also illustrate the typical arcuate detachment associated with the settlement problem under investigation (the same finding was also observed

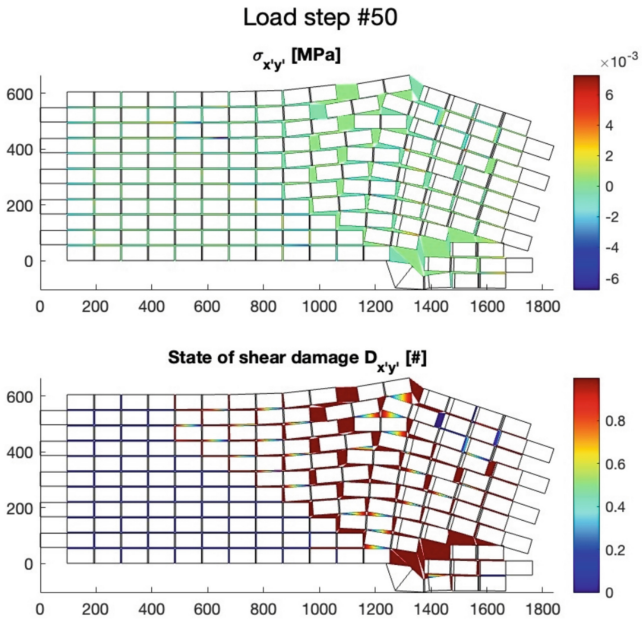


Fig. 9. Local behavior (step #50). Tangential stresses and state of shear damage.

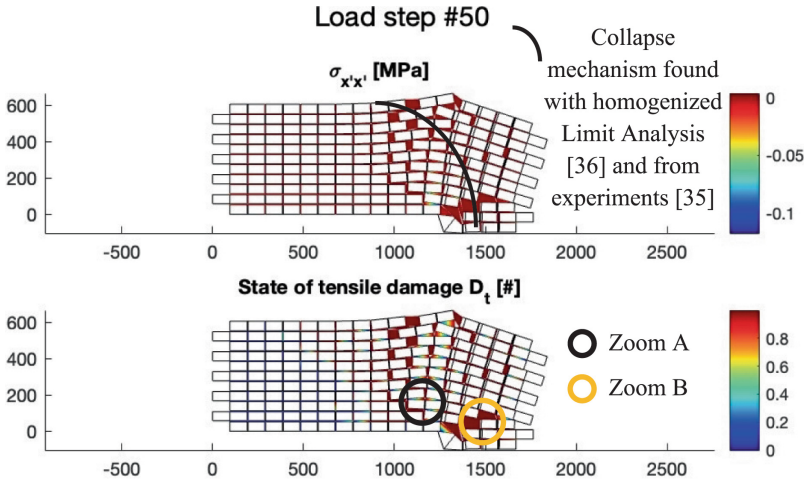


Fig. 10. Local behavior (step #50). Normal stresses and state of tensile damage.

in [35, 36]). Finally, in Fig. 12, zoom B from Fig. 10 is compared with the physical outcome.

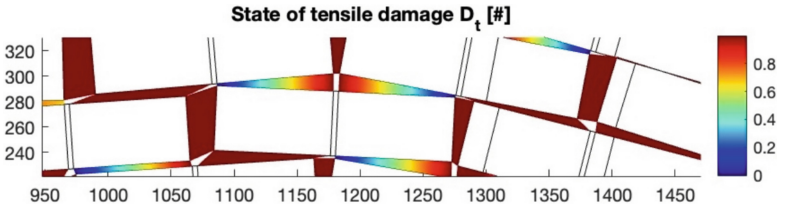


Fig. 11. Local behavior (step #50). State of tensile damage (zoom A, see Fig. 10).

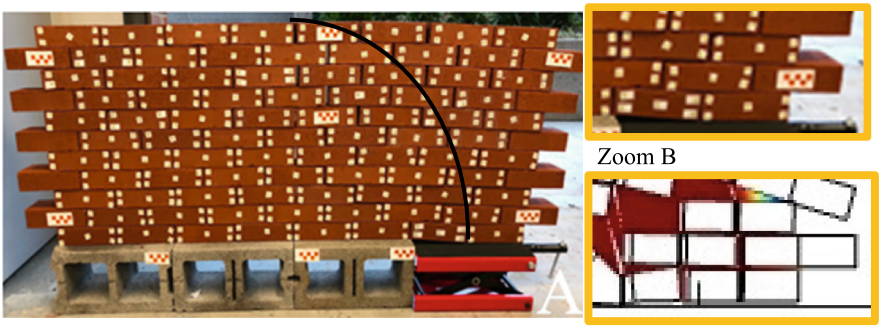


Fig. 12. Experimental results found in [35]. On the right, zoom B is compared with the outcome from [35] (zoom B, see Fig. 10).

4 Conclusions

The preliminary results obtained using FEMANOLA v3.0, an in-house developed non-linear FE software designed for robust anelastic static analyses of in-plane loaded masonry structures, have been presented. The software incorporates several key features that distinguish it from conventional approaches: (i) a heterogeneous modeling strategy that explicitly represents both bricks and mortar joints; (ii) mortar joints represented as interfaces with thickness, where all non-linearity is concentrated; (iii) bricks considered as elastic; (iv) mortar interfaces modeled with a single row of four-noded isoparametric elements, assuming a diagonal stiffness matrix and a vanishing elastic modulus along the interface direction; (v) a constitutive model incorporating a coupling between inelastic shear behavior and normal stress at the interface level.

Non-linearity is handled through a progressive penalization of the elastic moduli at Gauss points exhibiting softening during a given loading step. This approach results in a fully explicit and computationally efficient algorithm, eliminating the need for iterative solvers while maintaining numerical stability. The constitutive behavior follows a sawtooth law, ensuring a clear and controlled evolution of material degradation under loading conditions.

The computational cost required for the case study under investigation is approximately 3 min on a standard laptop. However, it is important to note that comparing computational times can be challenging, as software that generates figures, as the present

version does, for example, cannot be directly compared to others that do not offer this feature.

The proposed model provides a significant amount of detailed information, particularly at the local scale, compared to other numerical methods in the literature. This feature is especially useful for capturing crack initiation, propagation, and failure mechanisms in masonry subjected to settlements. The accuracy of the numerical results was validated against both numerical and experimental data available in the literature, with a specific benchmark test involving a masonry wall subjected to soil settlements. The model demonstrated excellent predictive capabilities, effectively replicating both the global structural response and local behavior.

Beyond the specific validation case, FEMANOLA v3.0 represents a promising tool for assessing the structural integrity of masonry buildings affected by 2D loading conditions. Its ability to explicitly model heterogeneous masonry, coupled with a computationally efficient nonlinear solver, makes it a valuable resource for both research and practical engineering applications. Future developments will aim to further enhance the software capabilities, including the integration of arc-length control techniques to improve the robustness of softening simulations and the extension of the methodology to three-dimensional problems. Additionally, the potential coupling of the model with soil-structure interaction analyses could further improve its applicability in engineering practice, offering more comprehensive assessments of masonry behavior under various loading conditions. Moreover, future work will include the development of scaled models fabricated using additive manufacturing techniques, allowing for more controlled experimental validation and deeper insights into the mechanical response of masonry structures. Another important aspect of future development is the creation of a graphical user interface (GUI), which will simplify the interaction with the software and make its use more accessible to engineers and researchers alike.

Acknowledgments. The study was partially developed within the research activities carried out in the frame of 2024–2026 ReLUIS Project – WP10 masonry structures (Coordinator – Prof. Guido Magenes), specifically by means of the research carried out in WP10.1.1 and WP10.2 Masonry Structures (Task Coordinators – respectively Prof. Serena Cattari and Prof. Sergio Lagomarsino). The Italian Department of Civil Protection has funded such a project. Finally, the study was partially developed with the financial support of the Italian Ministry of Scientific Research MUR within the research project PRIN-2022 (https://www.dabc.polimi.it/en/progetto/advanced-mechanical-models-and-computational-methods-for-large-scale-3d-printing-of-innovative-concrete-structures/) titled “Advanced mechanical models and computational methods for large-scale 3D printing of innovative concrete structures (COM^3D-CREATE)” (National PI: Prof. Andrea Chiozzi, Local PI: Prof. Gabriele Milani). Finanziato dall’Unione europea – Next Generation EU, Missione 4 Componente 1 CUP D53D23004070006.

Disclosure of Interests. The authors have no competing interests to declare that are relevant to the content of this article.

References

1. Buzzetti, M., Pingaro, N., Milani, G.: Automatic detection of local collapse mechanisms in historical masonry buildings: Fast and robust FE upper bound limit analysis. Eng. Fail. Anal. **170**, 109310 (2025)
2. Pingaro, N., Tiberti, S., Milani, G.: Automatic CAD kinematic limit analysis approach for the limit analysis of masonry towers. In: Simos T. (ed.) Proceedings of the 17th International Conference of Numerical Analysis and Applied Mathematics, ICNAAM 2019, Rhodes, Greece (2019)
3. Pingaro, N., Milani, G.: Full 3D CAD procedure for the speedy evaluation of the seismic vulnerability of masonry towers. In: In: Simos T. (ed.) Proceedings of the 15th International Conference of Computational Methods in Sciences and Engineering, ICCMSE 2019, Rhodes, Greece (2019)
4. Pingaro, N., Milani, G.: Simple non-linear numerical modelling of masonry arches reinforced with SRG using elasto-fragile and elasto-ductile truss finite elements. Eng. Struct. **293**, 116637 (2023)
5. Pingaro, N., Buzzetti, M., Milani, G.: Advanced FE nonlinear numerical modeling to predict historical masonry vaults failure: assessment of risk collapse for a long span cloister vault heavily loaded at the crown by means of a general-purpose numerical protocol. Eng. Fail. Anal. **167**, 109070 (2025)
6. Gandolfi, A., Pingaro, N., Milani, G.: Simple nonlinear numerical modeling for unreinforced and FRP-reinforced masonry domes. Buildings **14**(1), 166 (2024)
7. Gandolfi, A., Pingaro, N., Milani, G.: Elastic Body Spring Method (EBSM) for the stability analysis of the Global Vipassana Pagoda in Mumbai, India. Buildings **15**, 653 (2025)
8. Pourfouladi, M., Pingaro, N., Valente, M.: PoliBrick plugin as a parametric tool for digital stereotomy modelling. Comput. Struct. **311**, 107722 (2025)
9. Como, M.: Settlement response of masonry constructions. In: Geotechnical Engineering for the Preservation of Monuments and Historic Sites – Proceedings of the 2nd International Symposium on Geotechnical Engineering for the Preservation of Monuments and Historic Sites, Naples, Italy, pp. 265–272 (2013)
10. Iannuzzo, A., Mallardo, V.: A novel approach to model differential settlements and crack patterns in masonry structures. Eng. Struct. **323**, 119220 (2025)
11. Iannuzzo, A., Musone, V., Ruocco, E.: A neural network-based automated methodology to identify the crack causes in masonry structures. Comput. Aided Civil Infrastruct. Eng. **39**(24), 3769–3785 (2024)
12. Prosperi, A., Longo, M., Korswagen, P.A., Korff, M., Rots, J.G.: Sensitivity modelling with objective damage assessment of unreinforced masonry façades undergoing different subsidence settlement patterns. Eng. Struct. **286**, 116113 (2023)
13. Como, M.: Statics of Historic Masonry Constructions, 2nd edn. Springer, Berlin (2013)
14. Burd, H.J., Houlsby, G.T., Augarde, C.E., Liu, G.: Modelling tunnelling-induced settlement of masonry buildings. In: Proceedings of the Institution of Civil Engineers – Geotechnical Engineering, vol. 143, no. 1, pp. 17–29 (2000)
15. Giardina, G., Marini, A., Hendriks, M.A.N., Rots, J.G., Rizzardini, F., Giuriani, E.: Experimental analysis of a masonry façade subject to tunnelling-induced settlement. Eng. Struct. **45**, 421–434 (2012)
16. Giardina, G., van de Graaf, A.V., Hendriks, M.A.N., Rots, J.G., Marini, A.: Numerical analysis of a masonry façade subject to tunnelling-induced settlements. Eng. Struct. **54**, 234–247 (2013)
17. Zampieri, P., Zanini, M.A., Faleschini, F., Hofer, L., Pellegrino, C.: Failure analysis of masonry arch bridges subject to local pier scour. Eng. Fail. Anal. **79**, 371–384 (2017)

18. Alessandri, C., Garutti, M., Mallardo, V., Milani, G.: Crack patterns induced by foundation settlements: integrated analysis on a renaissance masonry palace in Italy. Int. J. Architect. Herit. **9**(2), 111–129 (2015)
19. Reccia, E., Milani, G., Cecchi, A., Tralli, A.: Full 3D homogenization approach to investigate the behavior of masonry arch bridges: the Venice trans-lagoon railway bridge. Constr. Build. Mater. **66**, 567–586 (2014)
20. Lemos, J.V.: Discrete element modelling of masonry structures. Int. J. Architect. Herit. **1**(2), 190–213 (2007)
21. Bui, T.T., Limam, A., Sarhosis, V., Hjiaj, M.: Discrete element modelling of the in-plane and out-of-plane behaviour of dry-joint masonry wall constructions. Eng. Struct. **136**, 277–294 (2017)
22. Zampieri, P., Simoncello, N., Pellegrino, C.: Structural behaviour of masonry arch with no-horizontal springing settlement. Fract. Struct. Integr. **12**(43), 182–190 (2018)
23. Galassi, S., Zampieri, P.: A new automatic procedure for nonlinear analysis of masonry arches subjected to large support movements. Eng. Struct. **276**, 115359 (2023)
24. Portioli, F., Cascini, L.: Assessment of masonry structures subjected to foundation settlements using rigid block limit analysis. Eng. Struct. **113**, 347–361 (2016)
25. Grillanda, N., Mallardo, V.: Compatible strain-based upper bound limit analysis model for masonry walls under in-plane loading. Comput. Struct. **313**, 107743 (2025)
26. Galassi, S.: An alternative approach for limit analysis of masonry arches on moving supports in finite small displacements. Eng. Fail. Anal. **145**, 107004 (2023)
27. Portioli, F., Cascini, L.: Large displacement analysis of dry-jointed masonry structures subjected to settlements using rigid block modelling. Eng. Struct. **148**, 485–496 (2017)
28. Iannuzzo, A., et al.: Modelling the cracks produced by settlements in masonry structures. Meccanica **53**(7), 1857–1873 (2018)
29. Iannuzzo, A., Block, P., Angelillo, M., Gesualdo, A.: A continuous energy-based numerical approach to predict fracture mechanisms in masonry structures: CDF method. Comput. Struct. **257**, 106645 (2021)
30. Pari, M., Van de Graaf, A.V., Hendriks, M.A.N., Rots, J.G.: A multi-surface interface model for sequentially linear methods to analyse masonry structures. Eng. Struct. **238**, 112123 (2021)
31. Yu, C., Hoogenboom, P., Rots, J.: Extension of incremental sequentially linear analysis to geometrical non-linearity with indirect displacement control. Eng. Struct. **229**, 111562 (2021)
32. Pari, M., Swart, W., Gijzen, M., Hendriks, M.A.N., Rots, J.G.: Two van solution strategies to improve the computational performance of sequentially linear analysis for quasi brittle structures. Int. J. Numer. Meth. Eng. **121**, 2128–2146 (2020)
33. Pingaro, N., Milani, G.: A novel analytical model for fiber reinforced cementitious matrix FRCM coupons subjected to tensile tests. Compos. Struct. **327**, 117666 (2024)
34. Pingaro, N., Calabrese, A.S., Milani, G., Poggi, C.: Debonding sawtooth analytical model and FE implementation with in-house experimental validation for SRG-strengthened joints subjected to direct shear. Compos. Struct. **319**, 117113 (2023)
35. Napolitano, R., Glistic, B.: Methodology for diagnosing crack patterns in masonry structures using photogrammetry and distinct element modelling. Eng. Struct. **181**, 519–528 (2019)
36. Tiberti, S., Grillanda, N., Mallardo, V., Milani, G.: A genetic algorithm adaptive homogeneous approach for evaluating settlement-induced cracks in masonry walls. Eng. Struct. **221**, 111073 (2020)